Isomerization of Azo Compounds. Cleavage Recombination Mechanism of Azosulfides

ARTICLE *in* THE JOURNAL OF PHYSICAL CHEMISTRY A · JUNE 1999

Impact Factor: 2.69 · DOI: 10.1021/jp990418n

Isomerization of Azo Compounds. Cleavage Recombination Mechanism of Azosulfides

Philippe Guiriec,[†] Philippe Hapiot,[†] Jacques Moiroux,[†] Andreas Neudeck,[‡] Jean Pinson,*[,†] and Cinzia Tavani[§]

Laboratoire d'Electrochimie Moléculaire de l'Université Paris 7, Unité Mixte de Recherche Université—CNRS no. 7591, Université Paris 7-Denis Diderot, 2 Place Jussieu, F-75251 Paris Cedex 05, France, IFW Dresden, Institut für Festkörperforschung, Abteilung Elektrochemie und leitfähige Polymere, Helmholtzstrasse 20, D-01069 Dresden, Germany, and Dipartimento di Chimica e Chimica Indutsriale, C.N.R., Centro di Studio per la Chimica dei Composti Cicloalifatici e Aromatici, Universita di Genova, Via Dodecaneso 31, I-16146 Genova, Italy

Received: February 4, 1999; In Final Form: April 21, 1999

(*Z*)-4-Nitrophenyl *tert*-butylsulfide [(*Z*)-4-NO_2−**1**], upon formation of its radical anion, isomerizes to the (*E*)-isomer at a very fast rate of 6.3×10^6 s^{-1}, about 10^3 times faster than azobenzene, while the 4-fluoro *tert*-butylsulfide (4-F−**1**) cleaves without isomerization. The particular behavior of 4-NO_2−**1** is related to the occurrence of a cleavage recombination mechanism, different from the usual inversion rotation mechanism. The existence of a reversible cleavage for the radical anion of 4-NO_2−**1** bears consequences on the mechanism of $S_{RN}1$ reactions of azosulfides; the attack of the nucleophile would take place on the intermediate diazenyl radical and not on the ensuing aryl radical as previously proposed.

Introduction

Azo compounds can exist as cis-(*Z*)- or trans-(*E*) isomers depending on the stereochemistry around the N═N double bond. Interconversion between these isomers can be achieved photochemically, thermally, or electrochemically. Photoisomerization of azobenzenze and its derivatives has received considerable attention over the past few years because of potential applications in areas such as high-density optical memory elements[1−3] and molecular switching devices.[4,5] Chemical binding of a photochrome to a redox group permits modulation of the electrochemical properties by an optical signal and therefore provides a chemical transducer.[6−17]

The cis ⇌ trans isomerization of azobenzene and its derivatives, which takes place in solution and solid-state thin films, is a first-order reaction that shows high quantum yields upon UV or blue light irradiation.[18] Owing to the overlap of the spectra of the cis and trans compounds, photochemistry leads to the establishment of photostationary states composed of a mixture of isomers.[19] Three possible cis ⇌ trans isomerization mechanisms have been discussed: (a) twisting around the N═N double bond (rotation mechanism) and (b) planar twist of one or (c) both of the σ bonds (inversion mechanism; Scheme 1). On the basis of ab initio calculations[20] of excited state potential energy surfaces, mechanim c has been excluded as energetically unfavorable in the case of diimine and azomethane. Quantum mechanical calculations on azobenzene itself[21] found that different pathways could be followed depending on the excited state involved but that the inversion mechanism b is the favored one at the level of the S_1 excited state. This was later demonstrated[22] through a femtosecond investigation of the photoisomerization of *cis*-azobenzene, a very fast process that takes place in 170 fs. Observation of an isomerization in azobenzenophanes,[20] the stereochemistry of which prevents the occurrence of the rotation mechanism, provided a clear demonstration of the occurrence of an inversion mechanism b.

SCHEME 1

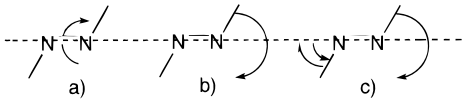

The cis ⇌ trans isomerization of nitrogen−nitrogen double bonds can also be induced thermally. It takes place[23] with an activation barrier of 84−105 kJ/mol and evidence has been provided both for the rotation[23−29] and for inversion.[30−35] Quantum mechanical calculations predict that the inversion path should be the preferred one.[21]

The electrochemical isomerization of N═N double bonds of azobenzene,[36,37] azocyclohexanes,[38] and azonorbornanes[39] has been much less investigated. Cyclic voltammetry (with several cycles) has permitted the demonstration[37] of the electrocatalytic conversion of the (*Z*)-isomer of azobenzene into the (*E*)-isomer and the differentiation between the two isomers; at a scan rate of 10 V/s, the peak of the (*Z*)-isomer is 60 mV more negative than that of the (*E*)-isomer. It was thus possible to measure the lifetime of the (*Z*)-radical anion (0.1 ms) as well as the activation energy of the reaction (8 kJ/mol). The related electrochemical isomerization around a C═C double bond has also been scrutinized in stilbenes,[40−43] dialkyl maleates,[44] and thioindigo.[45] Enol ethers[46] and 1,2-diarylsulfonylphenylethylenes[47] also undergo an electrochemically catalyzed isomerization with a rather low rate, since the two isomers can be distinguished at scan rates of, respectively, 10 and 0.1 V s^{-1}. In each case, the C═C isomerization of the cis to the trans compound takes place through the stereomutation of the radical anion formed upon electron addition. The rate constants that have been measured are relatively small, on the order of a few s^{-1} reaching 100 s^{-1} only in the case of dibenzoyl ethylene.

The intimate mechanism of the electrochemical isomerization of C═C or N═N double bonds at the level of the radical anion

[†] Université Paris 7.
[‡] Institut für Festkörperforschung.
[§] Universita di Genova.

10.1021/jp990418n CCC: $18.00
Published on Web 06/25/1999

(rotation or inversion) has never been investigated, but as in the photochemical isomerization, the three mechanisms mentioned above can be taken into account, the difference being that a radical anion is involved instead of an excited state.

Aryl azosulfides, which possess a sulfur atom bonded to the N=N double bond, can also exist in two isomeric forms:

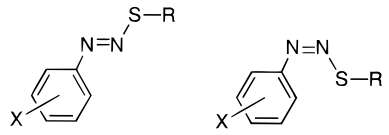

(E)-isomer *(Z)*-isomer

1: R = *tert*-butyl

Coupling of a diazonium ion with phenyl sulfide furnishes the (*E*)-isomer, while reaction with *tert*-butylsulfide provides the (*Z*)-isomer.[48] The (*E*)-aryl *tert*-butylsulfide can be prepared from the (*Z*)-isomer by heating, for example, in a nonpolar solvent.[48−51] Photochemical irradiation of the (*E*)-isomers leads to the formation of the (*Z*)-isomer.[49] More recently,[52] it was shown that irradiation of any of the (*Z*)- or (*E*)- isomer of 4-nitrophenylazo *tert*-butylsulfide (with a xenon lamp) leads to the formation of the other isomer and then to the cleavage of the molecule. When fast cyclic voltammetry and spectroelectrochemistry were combined, the (*Z*) to (*E*) electrocatalytic isomerization of 4-nitro- and 4-cyanophenyl azosulfides was observed, and it was possible to measure the high rate of this isomerization[52] (respectively, 6.3×10^6 and 4.0×10^6 s^{-1}). This rate constant is about 3 orders of magnitude larger than that of azobenzene; it was therefore interesting to find out where this large difference could come from. It is the aim of this paper to determine the mechanism: inversion, rotation, or the occurrence of a completely different mechanism. We will show that a mechanism involving the reversible cleavage of the radical anion to a radical and an anion followed by a recombination is operative.

The electrochemical isomerization of azosulfides takes place at the level of the radical anion. This radical anion can also be the starting point of $S_{RN}1$ reactions. Therefore, the electrochemically induced isomerization and the electrocatalytic $S_{RN}1$ reaction[53−56] are intimately interconnected, and it is not possible to discuss them separately. $S_{RN}1$ reactions of azosulfides have been used for the synthesis of a number of variously functionalized aromatic compounds with suitable anionic nucleophiles (Nu^-),[48,57−61] and the mechanism can be summarized as follows.

The $\mathbf{1}^{\bullet-}$ radical anion, obtained via cathodic or homogeneous reduction (e.g., by the nucleophile itself, sometimes under photostimulation; reaction 0), has been proposed to cleave (reaction 1) to eventually give nitrogen, thiolate, and an aryl radical; coupling between $Ar^\bullet$ and the nucleophile generates (reaction 2) the radical anion of the substitution product, which effectively closes the propagation cycle by means of an electron exchange with the substrate (reaction 3).

$$\underset{\mathbf{1}}{\text{ArN=NSR}} + \text{electron donor} \leftrightarrows \underset{\mathbf{1}^{\bullet-}}{\text{ArN=NSR}^{\bullet-}} \quad (0)$$

$$\underset{\mathbf{1}^{\bullet-}}{\text{ArN=NSR}^{\bullet-}} \xrightarrow{k_1} \text{Ar}^\bullet + \text{N}_2 + {}^-\text{SR} \quad (1)$$

$$\text{Ar}^\bullet + \text{Nu}^- \xrightarrow{k_2} \text{ArNu}^{\bullet-} \quad (2)$$

$$\text{ArNu}^{\bullet-} + \text{ArN=NSR} \leftrightarrows \text{ArNu} + \underset{\mathbf{1}^{\bullet-}}{\text{ArN=NSR}^{\bullet-}} \quad (3)$$

Anyway, the "external" nucleophile (Nu^-) always suffers competition by RS^- (i.e., the "internal" nucleophile, formed along the fragmentation step 1), whose coupling with $Ar^\bullet$ (reaction 4) triggers an alternative propagation cycle leading to the ArSR sulfide **2**.

$$\text{Ar}^\bullet + {}^-\text{SR} \xrightarrow{k_4} \text{ArSR}^{\bullet-} \quad (4)$$

$$\text{ArSR}^{\bullet-} + \text{ArN=NSR} \leftrightarrows \text{ArSR} + \underset{\mathbf{2}}{\text{ArN=NSR}^{\bullet-}} \quad (5)$$

By means of electrochemistry, which has proved to be a very efficient way of initiating and analyzing $S_{RN}1$ processes,[55,56,62−64] it has been possible to demonstrate that reaction 4 takes place in a solvent cage.[65,66]

In the absence of nucleophile, or in the case where reactions 2 and 4 are not efficient enough, the aryl radical $Ar^\bullet$ yields the corresponding aromatic ArH either by electron transfer and protonation by residual proton donors (reactions 6 and 7) or by hydrogen atom abstraction from the solvent[68,69](reaction 8).

$$\text{Ar}^\bullet + \text{electron donor} \leftrightarrows \text{Ar}^- \quad (6)$$

$$\text{Ar}^- + \text{residual proton donor} \leftrightarrows \text{ArH} \quad (7)$$

$$\text{Ar}^\bullet + \text{SH (solvent)} \rightarrow \text{ArH} + \text{S}^\bullet \quad (8)$$

In this paper, we will try to demonstrate that a cleavage recombination mechanism different from inversion b or rotation is operative in the isomerization of azosulfides, and we will discuss its consequences on the $S_{RN}1$ reactions of arylazosulfides. For this purpose we have investigated both by spectroelectrochemistry and by cyclic voltammetry a series of arylazo *tert*-butylsulfides (**1**). The azosulfides will be termed by the position and name of the aryl (Ar) substituents, for example, 4-NO_2−**1**, and the final products **2** by that of the two substituents, for example, 1-SBu^t-4-NO_2−**2**.

Results

The results of the slow scan rate cyclic voltammetry of azosulfides **1** are shown in Table 1, and two examples, 4-NO_2−**1** and 4-F−**1**, will be emphasized.

The voltammogram[52] of 4-NO_2-**1** has been already described (Figure 1). It consists, for both isomers, of a reversible one-electron wave (I) located at $E_p(Ic) = -0.95$ V/SCE, followed by a second two-electron wave leading to the radical anion of nitrobenzene. The voltammogram (Figure 2) of the two isomers of 4-F−**1** is completely different; it consists, for both isomers, of a single irreversible wave (Ic) located at $E_p(Ic) = -1.70$ V/SCE for the (*E*)-isomer and $E_p(Ic) = -1.79$ V/SCE for the (*Z*)-isomer. This wave shifts with the scan rate by a value close to 30 mV/log υ, which indicates a first-order reaction following a first electron transfer. The number of electrons transferred at the level of this wave is 1.1 for the (*E*)-isomer and the (*Z*)-isomer. The voltammetric characteristics of the different azosulfides are summarized in Table 1.

When the scan rate is increased, different behaviors can be observed. As indicated above, the voltammograms of (*E*)- and (*Z*)-4-NO_2−**1** are reversible at 0.2 V s^{-1}. That of the (*E*)-isomer remains reversible up to the high scan rates (12 000 V s^{-1}), while that of the (*Z*)-isomer at the same scan rate shows the cathodic peak pertaining to the (*Z*)-isomer on the forward cathodic scan and the anodic peak of the (*E*)-isomer on the reverse scan (Figure 1). This behavior was assigned[52] to the

TABLE 1: Cyclic Voltammetry Characteristics of Azosulfides[a,b]

azosulfide	(*E*) or (*Z*)	E_p(Ic)	*n*(Ic)	$E°$	k (s^{-1})	reversibility[c] of Ic
4-NO_2−**1**	(*E*)[d]	−0.95	1	−0.92	4.1×10^{-2}	R at $v = 0.2$ V s^{-1}
	(*Z*)	−0.95	1	−1.12		R at $v = 0.2$ V s^{-1}
3-NO_2−**1**	(*E*)	−1.09	1	−1.04	*e*	R at $v = 0.2$ V s^{-1}
	(*Z*)	−1.09	1	−1.02		R at $v = 0.2$ V s^{-1}
4-CN **1**	(*E*)	−1.31	0.81	−1.29	*e*	R at $v > 500$ V s^{-1}
	(*Z*)	−1.27	0.81	−1.16		R at $v > 500$ V s^{-1}
4-F−**1**	(*E*)	−1.70	1.10	−1.69	$\sim 2 \times 10^3$	R at $v > 1000$ V s^{-1} [f]
	(*Z*)	−1.79	1.10	*g*	$> 8.4 \times 10^5$	I up to 42000 V s^{-1} [f]
3-F−**1**	(*E*)	−1.58	0.70	−1.57	$\sim 6 \times 10^3$	R at $v > 1500$ V s^{-1} [f]
	(*Z*)	−1.67	0.65	*g*	$> 3.2 \times 10^5$	I up to 16000 V s^{-1} [f]
4-H−**1**	(*E*)	−1.69	0.91	−1.70	$\sim 4 \times 10^3$	R at $v > 1000$ V s^{-1} [f]
	(*Z*)	−1.76	0.97	*g*	$> 7.4 \times 10^5$	I up to 37000 V s^{-1} [f]
Me_3−**1**[h]	(*Z*)	−1.92	1.00	*g*	$> 3.5\ 10^5$	I up to 17500 V s^{-1} [f]
4-Bu^t−**1**	(*E*)	−1.72	0.4	−1.75	$\sim 0.5 \times 10^3$	R at $v > 1500$ V s^{-1} [f]
	(*Z*)	−1.85	0.83	*g*	$> 4.6 \times 10^5$	I up to 23000 V s^{-1} [f]
4-MeO−**1**	(*E*)	−1.65	1.00	−1.69	1×10^3	R at $v > 500$ V s^{-1} [f]
	(*Z*)	−1.68	0.87	*g*		I up to 500 V s^{-1} [f]

[a] In ACN + 0.1 M NBu_4BF_4, $c \approx 1$mM, glassy carbon electrode, $v = 0.2$ V s^{-1}, reference SCE. [b] E_p(Ic) is the peak potential of the first cathodic wave, *n*(Ic) the number of electrons transferred at the level of this peak, $E°$ the standard potential of this first electron transfer, k the cleavage rate constant of the radical anion of azosulfide. [c] R = reversible, I = irreversible. [d] The cleavage of this compound is equilibrated (see text), and the isomerization from (*Z*) to (*E*) is fast (ref 52). The cleavage is therefore that of the (*E*)-isomer). [e] See text. [f] On a 10 μm gold electrode. [g] Cannot be measured, since the reversibility cannot be obtained. [h] 2,4,6-trimethylphenylazo *tert*-butylsulfide.

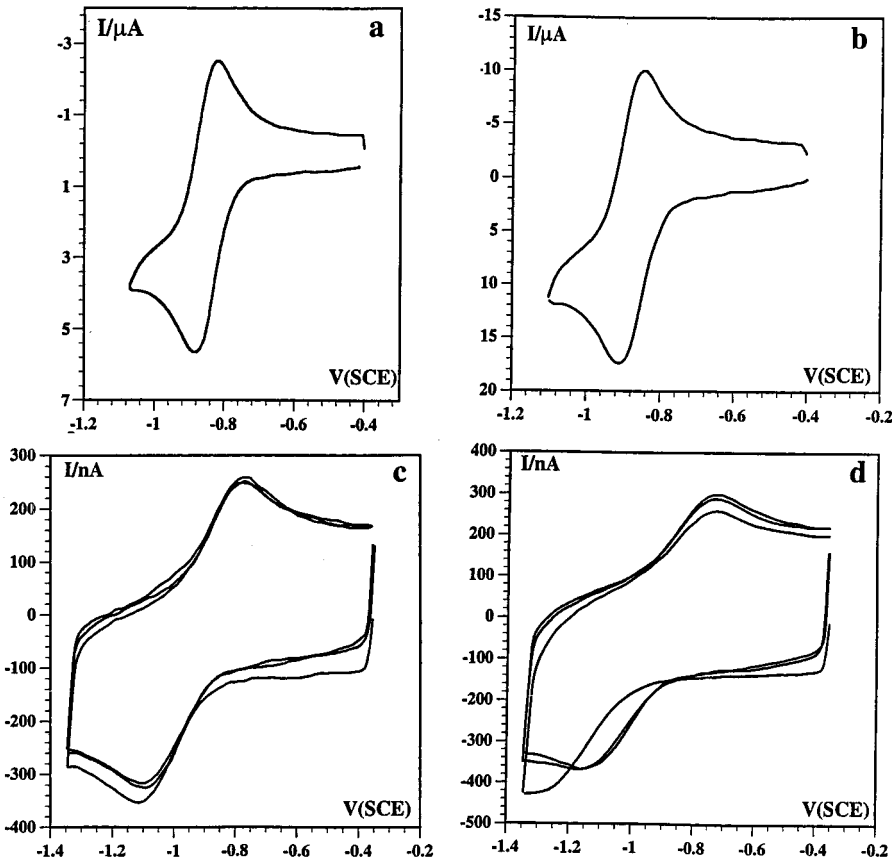

Figure 1. Cyclic voltammogram of (*E*)-4-NO_2−**1** (a,c) and (*Z*)-4-NO_2−**1** (b,d) at 0.2 (a,b) and 12 000 V s^{-1} (c,d). Glassy carbon electrode (a,b) and 15 μm gold electrode (c,d), reference SCE, solvent ACN + 0.1 M NBu_4BF_4 were used.

following mechanism with a fast isomerization, $k_{10} = 6.3 \times 10^6$ s^{-1} :

$$(Z)\text{-}\mathbf{1} + 1e^- \rightleftharpoons (Z)\text{-}\mathbf{1}^{\bullet -} \quad (9)$$

$$(Z)\text{-}\mathbf{1}^{\bullet -} \xrightarrow{k_{10}} (E)\text{-}\mathbf{1}^{\bullet -} \quad (10)$$

$$(E)\text{-}\mathbf{1}^{\bullet -} + (Z)\text{-}\mathbf{1}^{\bullet -} \rightleftharpoons (Z)\text{-}\mathbf{1}^{\bullet -} + (E)\text{-}\mathbf{1}^{\bullet -} \quad (11)$$

The cleavage of the radical anion is too slow to be observed by cyclic voltammetry even at the lowest scan rates. At this low scan rate, the isomerization has plenty of time to take place, while at high scan rate it is possible to outrun the isomerization process and to differentiate the two isomers.

With the 3-NO_2−**1** both isomers give identical reversible voltammograms at 0.2 V s^{-1}, but in contrast to the 4-analogue, the voltammograms remain closely similar up to 20 000 V s^{-1}. It is therefore not possible to show or to exclude an isomerization. The behavior[52] of 4-CN−**1** is similar to its nitro

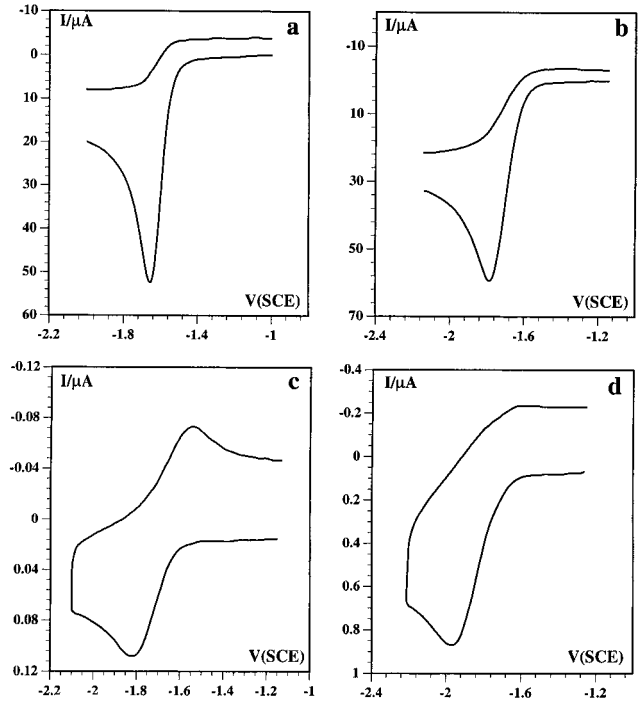

Figure 2. Cyclic voltammogram of (*E*)-4-F−**1** (a,c) and (*Z*)-4-F−**1** (b,d) at 0.1 (a,b) and 24 000 (c) and 27 000 V s^{-1} (d). Glassy carbon electrode (a,b) and 15 μm gold electrode (c,d), reference SCE, solvent ACN + 0.1 M NBu_4BF_4 were used.

analogue with the difference that with the rate of cleavage being larger, one starts at 0.2 V s^{-1} from a situation where the voltammograms of both isomers are irreversible and become reversible at scan rates of about 500 V s^{-1}, and at very high scan rates, one can distinguish between the two isomers. All the remaining azosulfides (4-F−**1**, 3-F−**1**, 4-H−**1**, 2,4,6-Me_3−**1**, 4-Bu^t−**1**, 4-MeO−**1**) present similar patterns (Figure 2): the low scan rate voltammograms are irreversible (because of the cleavage rate of the radical anion). When the scan rate is increased, the two isomers are differentiated; the (*E*)- isomer becomes reversible at 500−1500 V s^{-1}, while the (*Z*)-isomer always remains irreversible. This behavior and the difference of peak potentials at low scan rate clearly indicate that there is no fast isomerization taking place as observed previously[52] for 4-NO_2 and CN−**1**, and the differences between the voltammograms at 0.2 V s^{-1} only leave the possibility of a very slow isomerization, so slow that it could not take place during the time lapse of a few seconds necessary to record the voltammogram at 0.2 V s^{-1}. The rate constants *k* for the cleavage of the radical anions obtained by simulation[69] of the voltammograms, assuming a first-order reaction following the electron transfer, are gathered in Table 1.

As concerns 3-NO_2−**1**, cyclic voltammetry measurements leave some ambiguity on whether there is a fast or slow isomerization. This uncertainty can be relieved by spectroelectrochemistry, which also permits confirmation of the absence of isomerization for the azosulfides showing different voltammograms at high scan rate for the two isomers. Spectroelectrochemistry is a technique that permits the recording of successive UV−vis spectra of the solution close to the electrode while the potential is scanned. It has been recently improved by the use of gold LIGA structures (honeycombed microstructures with well-defined hexagonal holes in the range of a few micrometers), where transient species have been observed down to the millisecond range.[70−73] Figure 3 shows the spectrocyclovoltammogram of the two isomers of 3-NO_2−**1.** The (*Z*)-isomer presents a spectrum with an absorption at 304 nm; when the potential is scanned toward negative potentials, a new spectrum appears with maxima at 319 and 481 nm, which can be assigned to the radical anion 3-NO_2−$\mathbf{1}^{\bullet-}$. At the end of the cyclic voltammogram a new spectrum is obtained with a maximum at 327 nm. This last spectrum is identical to that of the (*E*)-isomer. If the same experiment is performed starting from the (*E*)- isomer, no change is observed between the initial and the final spectrum while the intermediate spectrum is very similar to that obtained from the (*Z*)- isomer. Therefore, the behavior of this 3-NO_2−**1** derivative is somewhat different from that of 4-NO_2−**1**, which has been previously observed, since for this last compound the spectrum of the (*E*)-isomer appeared at a potential of about 100 mV ahead of the voltammetric wave. As a result of the difference of reduction potential between isomers, the isomerization of 4-NO_2−**1** was electrocatalyzed, which is not the case for 3-NO_2−**1**. Therefore, at low scan rate, the (*Z*)-3-NO_2−**1** isomerizes to the (*E*)-isomer during the recording time of the spectrocyclovoltammogram (about 10 s). At high scan rate the voltammograms of the two isomers are very similar, the measured $\Delta E°$ being only 20 mV. This similarity of the voltammograms prevents any sound simulation to be performed and therefore the measurement of the isomerization rate constant.

A very different spectrocyclovoltammetry is observed starting from the 4-F−**1** (Figure 4). Starting from the (*Z*)-isomer (λ_{max} = 303 nm) or from the (*E*)-isomer (λ_{max} = 327 nm), one obtains the same final spectrum (λ_{max} = 297 nm) different from any of the starting isomers. An electrolysis was performed (see Experimental Section) to determine the final products among which one finds the 4-fluorophenyl *tert*-butylsulfide as well as products resulting from further reactions of this sulfide. The 4-fluorophenyl *tert*-butylsulfide absorbs at 217 nm with a shoulder at 260 nm (ϵ = 1300 L mol^{-1} cm^{-1}), and therefore, the absorption at 297 nm corresponds to the mixture of this sulfide and the products resulting from its further reactions.

In this case it is not possible to observe the intermediate radical anion (this could be expected in view of fact that the reversibility of the (*E*)-isomer is reached at scan rates higher than 1000 V s^{-1} and that of the (*Z*)-isomer cannot be observed up to 42 000 V s^{-1}). Therefore, both cyclic voltammetry and spectroelectrochemistry point to a cleavage of the molecule being faster than the isomerization from the (*Z*)-isomer to the (*E*)-isomer; as the voltammogram of the (*Z*)-isomer remains irreversible up to 42 000 V s^{-1}, one can estimate that the rate of cleavage of (*Z*)-4F−$\mathbf{1}^{\bullet-}$ is higher than 8.4×10^5 s^{-1}, a value that represents an upper limit for the rate of isomerization. The characteristics of the spectra are summarized in Table 2.

For compounds 4-H, 4-Bu^t, and 3-MeO−**1**, one can observe, on the spectrocyclovoltammogram of the (*Z*)-isomer before the potential where the final product is formed, a very minute amount of the (*E*)-isomer. For example, in the case of (*Z*)-4H−**1** (with λ_{max} at 306 nm) a shoulder appears at 327 nm, the maximum of the (*E*)-isomer before the formation of the final product (with λ_{max} at 299 nm).

From the above experiments the investigated azosulfides fall into three categories: 4-NO_2−**1**, 3-NO_2−**1**, and 4-CN−**1**, which cleave rather slowly, the (*Z*)- to (*E*)-isomerization, which is much faster than the cleavage, and 4-F−**1** and 3-F−**1**, which cleave faster and for which the isomerization is slower than the cleavage and cannot be observed. Compounds 4-H, 4-Bu^t, and 4-MeO−**1** fall between isomerization and cleavage; the cleavage is fast for the (*E*)-isomer and very fast for the (*Z*)-isomer, but a slow isomerization can be observed at a potential just before

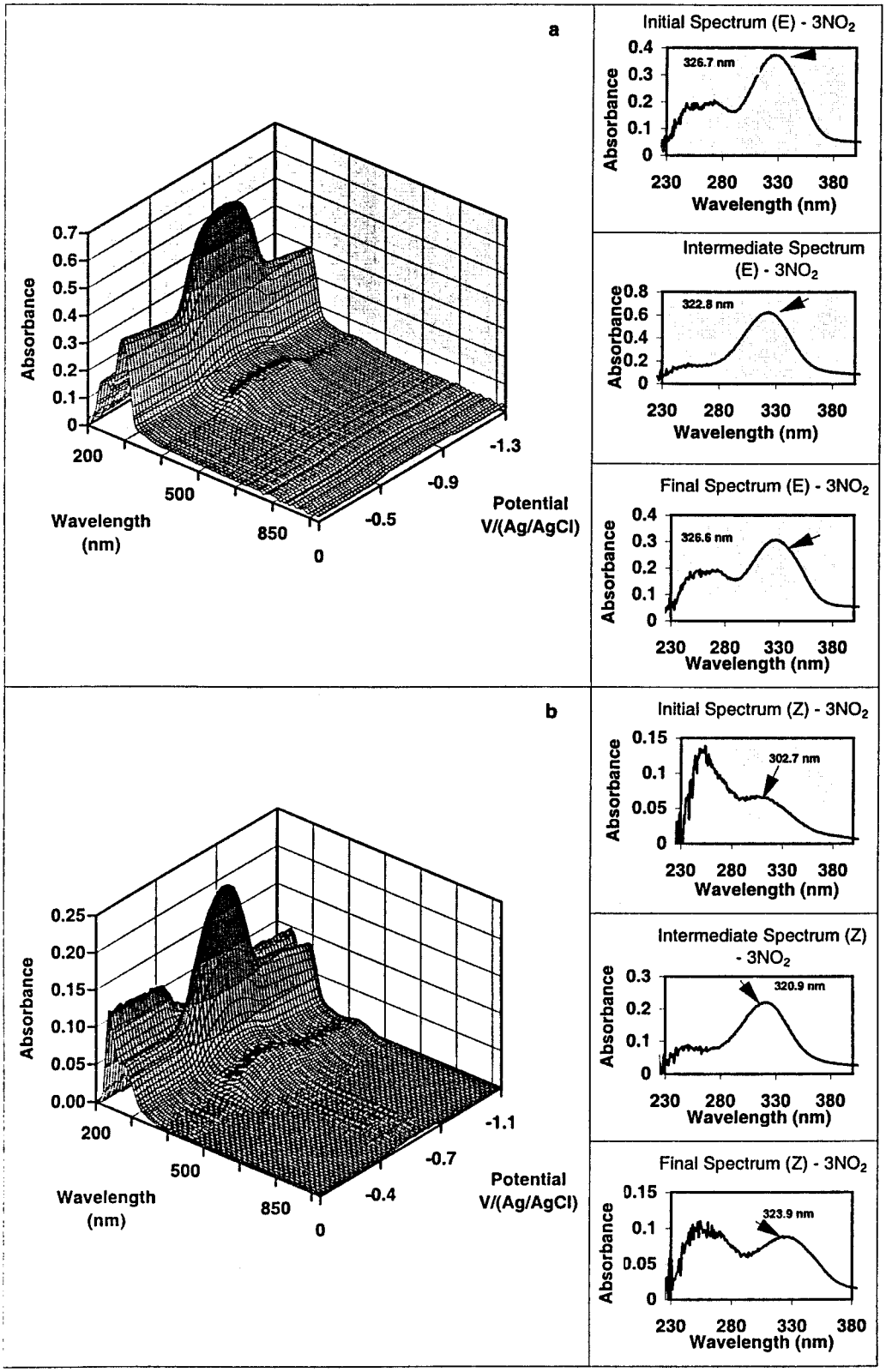

Figure 3. Absorbance wavelength−time plot of (*Z*)-3-NO_2−**1** and (*E*)-3-NO_2−**1** recorded in the gold LIGA cell. Solvent ACN + 0.1 M NBu_4BF_4 was used. Potentials scanned were the following: $0 \rightarrow -1.30 \rightarrow 0$ V SCE. $v = 0.4$ V s^{-1}. Insets show the initial, intermediate, and final spectra.

the cleavage occurs. The first category includes azosulfides with strong electron-withdrawing groups in the para and meta positions. Focusing our attention on the 4-nitro derivative, we tried to characterize the effect of the 4-NO_2 group on the electron density on the N═N bond and to find out if this change of spin density could favor a fast rotation (a) or inversion (b) mechanism. For this purpose we recorded the ESR spectrum[74] and calculated the spin densities of (*E*)-4-NO_2−$\mathbf{1}^{\bullet -}$.

The experimental and simulated ESR spectra[75,76] are shown in Figure 5. The simulation indicates the presence of three different nitrogen atoms ($a_{N[1]} = 0.525$ mT, $a_{N[2]} = 0.399$ mT, $a_{N[3]} = 0.134$ mT) and four hydrogen atoms ($a_{H[1]} = 0.305$ mT,

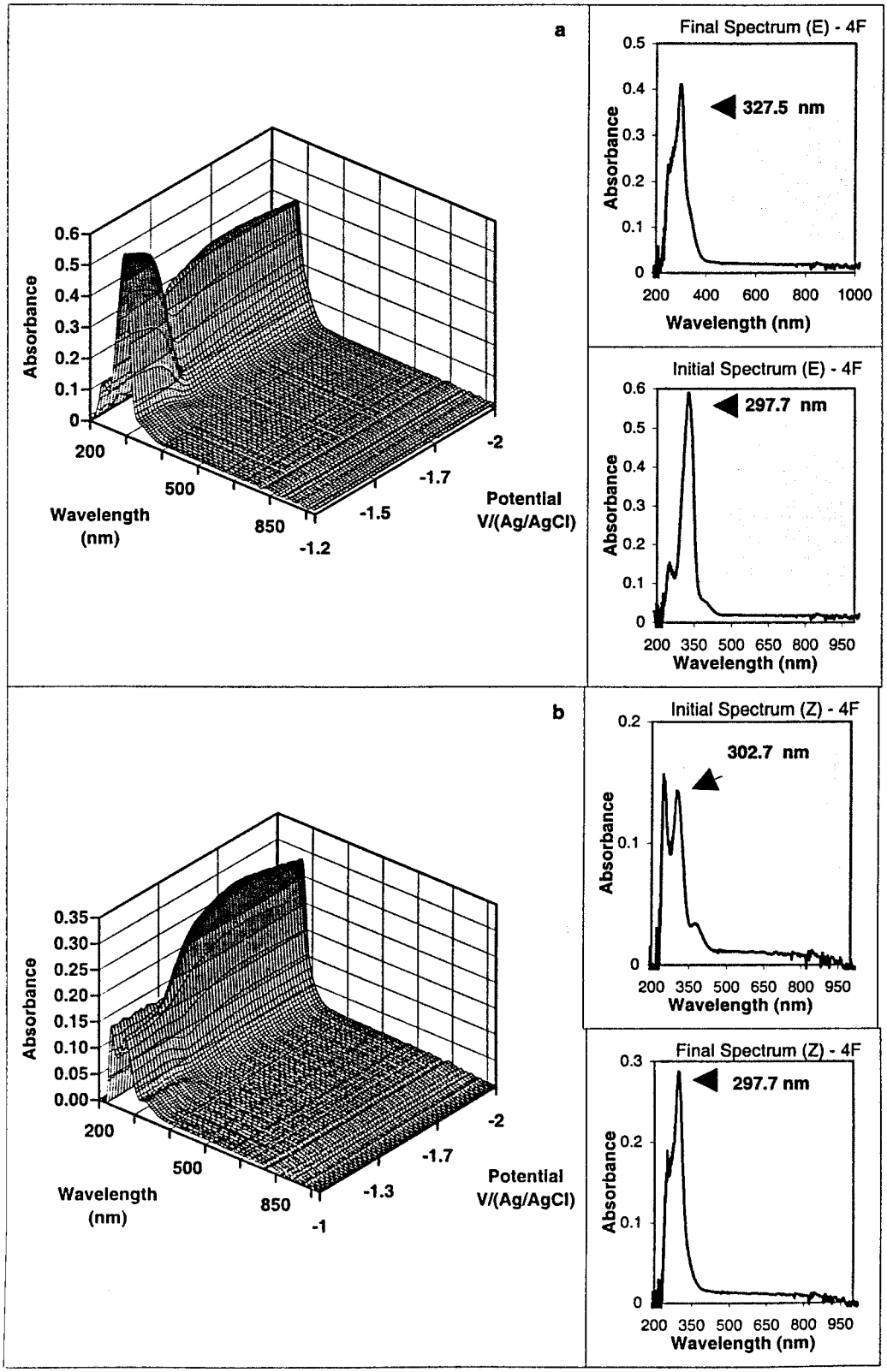

Figure 4. Absorbance wavelength−time plot of (*Z*)-4-F−**1** and (*E*)-4-F−**1** recorded in the gold LIGA cell. Solvent ACN + 0.1 M NBu_4BF_4 was used. Potentials scanned were the following: $0 \rightarrow -2.0 \rightarrow 0$ V SCE. $\nu = 0.3$ V s^{-1}. Insets show the initial and final spectra.

$a_{H[2]} = 0.254$ mT, $a_{H[3]} = 0.079$ mT, $a_{H[4]} = 0.079$ mT). Assignment of the coupling constants is detailed in Appendix 2 in Supporting Information; N[1] with the largest coupling constant would correspond to the nitrogen bonded to the sulfur atom, while N[2] would correspond to the other azo nitrogen and N[3] to that of the nitro group. In the case of nitro groups, the coupling constant has been shown to correlate linearly with the spin density on the nitrogen atom.[77] Comparison of the above value of $a_N = 0.134$ mT with the value of 1.032 mT for nitrobenzene itself and 1.218 mT for nitroaniline indicates a small spin density on the nitrogen of (*E*)-4-NO_2−**1**$^{\bullet-}$.

Calculations[78] were performed on the radical anions of (*E*)-4-NO_2−**1** and (*E*)-4-F−**1** using the density functional theory (B3LYP/6.31G*//B3LYP/6.31G*) to take into account the

TABLE 2: Spectral Findings of Azosulfides, Radical Anions, and Final Products[a]

azosulfides	$\lambda_{max}(E)$ (nm)	$\lambda_{max}(Z)$ (nm)	λ_{mas} (nm) radical anion	λ_{max} (nm) final spectrum
4-NO_2−**1**	345	305, 345[b]	458, 750[b] 850, 959	295, 350
3-NO_2−**1**	327	304	322, 488	327, 501
4-CN−**1**	331	300	426	292, 350
4-F−**1**	328	304, 377	*c*	297
3-F−**1**	329	301	*c*	299
4-H−**1**	327, 391[b]	306, 379[b]	*c*	299
4-Bu^t−**1**	330, 390[b]	312, 384[b]	*c*	298
3-MeO−**1**	329	309, 375[b]	*c*	299

[a] In ACN + 0.1 M NBu_4BF_4. [b] Shoulder. [c] Lifetime below detection limit.

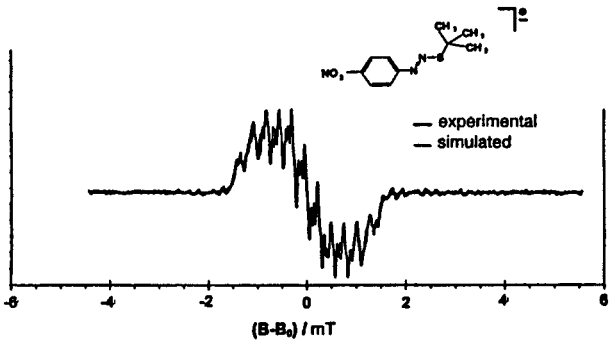

Figure 5. Experimental and calculated ESR spectrum of the radical anion (*E*)-4-NO_2−**1**$^{\bullet-}$.

TABLE 3: Calculated Spin Densities of the Radical Anions

	C1	N1[a]	N2[a]	S	N(NO_2)
(*E*)-4-NO_2−**1**$^{\bullet-}$ [b]	0.112	0.014	0.387	0.037	0.070
(*E*)-4-F−**1**$^{\bullet-}$ [c]	−0.028[d]	0.258	0.423	0.014	

[a] N1 is next to the phenyl ring, N2 next to the sulfur atom. [b] S^2 = 0.77. [c] S^2 = 0.76. [d] Negative value due to some spin contamination from higher states.

influence of electron correlation in the radical anion. The results are given in Table 3.

Comparison of the spin densities calculated for the nitro and fluoro radical anions shows that the nitro group shifts the spin density from the two nitrogens to C1 of the phenyl ring and to the NO_2 group, a shift that could favor an inversion (b) or rotation (a) mechanism. To confirm this point, we approximated the transition state of both an inversion (b) and a rotation (a) mechanism by calculating (by a semiempirical AM1 method) the energy of the radical anion with a linear N−N−S geometry (inversion mechanism b)) and with a N−S bond at 90° from the phenyl-N═N plane (rotation mechanism). In the three cases the rotation (a) is favored over the inversion (b) (by a change of ∼40 kJ/mol). Not unexpectedly, the result calculated for the radical anion is therefore different from what was previously calculated and measured for excited states.[21] Although not precise enough for quantitative predictions, the above estimations also indicate that the rotation mechanism should be faster for both 4-F and 4-NO_2−**1** than for azobenzene itself for which a rate of isomerization of approximately 7×10^3 s^{-1} has been previously measured.[37]

In view of the above experimental results and calculated estimations, which do not provide a clear rationale for the fast isomerization of 4-NO_2 and 4-CN **1** and for the absence of observable isomerization for 4-F−**1**, and since the isomerization problem is closely related to the mechanism of the $S_{RN}1$ reaction, we reexamined the kinetics of cleavage of 4-NO_2−**1** in the presence of nucleophiles. This rate of cleavage has been

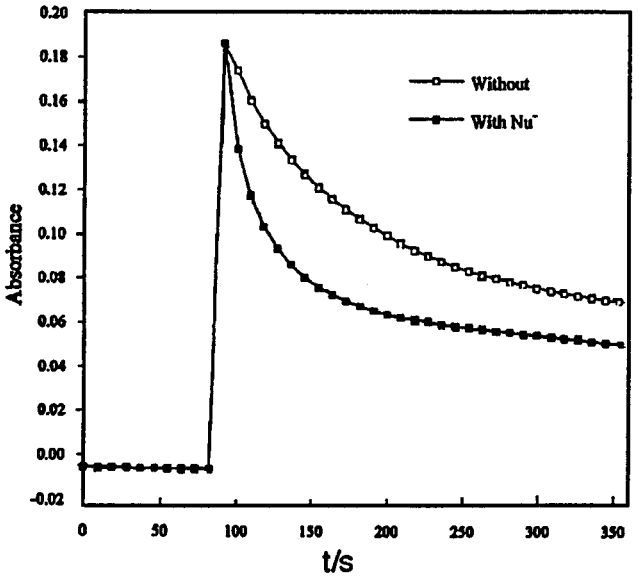

Figure 6. Decays of the spectrum of (*E*)-4-NO_2−**1**$^{\bullet-}$ at 850 nm, c^0-[(*E*)-**1**] = 2.44 mM, in absence (□) and in the presence (■) of NMe_4^+ $^-CH(CN)_2$ (c^0 = 80 mM).

measured by spectroelectrochemistry[52] following the decay of the spectrum of (*E*)-4-NO_2−**1**$^{\bullet-}$ at 850 nm. In the presence of a nucleophile, malononitrile anion NMe_4^+ $^-CH(CN)_2$, the decay of this radical anion becomes faster (Figure 6). The same phenomenon can be observed by cyclic voltammetry (Figure 7). At 200 mV/s, the voltammogram of 4-NO_2−**1** is reversible, and one measures i_{pa}/i_{pc} = 0.62 (the peak heights being measured from the baseline). Upon addition of a 0.1 M concentration of malononitrile anion, the reversibility decreases: i_{pa}/i_{pc} = 0.48. This loss of reversibility also appears, although of less intensity, with another nucleophile cyanide anion; i_{pa}/i_{pc} = 0.58 in the presence of 0.647 M CN^-. Both of these experiments can be interpreted as an $S_{RN}1$ reaction involving a reversible cleavage of 4-NO_2−**1**$^{\bullet-}$. Three different reaction paths can be taken into account for the formation of 1-$CH(CN)_2$−4-NO_2−**2**. The first one involves reactions 0, 12, 14, and 18 (Scheme 2), 0+12+14+18. Reaction 0 furnishes a radical anion that cleaves reversibly to a diazenyl radical and *t*-butanethiolate. This diazenyl radical is attacked by the malononitrile anion (reaction 14) to give the radical anion of the substituted product. This radical anion can be reoxidized in solution by the starting azosulfide to give the final product 1-$CH(CN)_2$−4-NO_2−**2** (reaction 18) (in ACN this compound exists mainly as its conjugated anion[79]). This reaction pathway can be termed "reversible nonclassical $S_{RN}1$", nonclassical in the sense that the attack of the nucleophile occurs on the diazenyl radical and not on the aryl radical. The attack of the nucleophile on the diazenyl radical would be in competition with the attack of *t*-butanethiolate: "the internal nucleophile" (reaction 13) and the cleavage of this diazenyl radical (reaction 15). A second reaction path is described by reactions 0, 12, 15, 16, and 18, 0+12+15+16+18; the diazenyl radical formed as above cleaves to give an aryl radical that reacts with the nucleophile to give the radical anion of the substituted product (this is a "reversible classical $S_{RN}1$" reaction, classical in the sense that the nucleophile attacks the aryl radical). Finally, the *t*-butanethiolate can also react with the nitrophenyl radical to ultimately give 4-nitrophenyl *tert*-butylsulfide (reactions 17 and 19, 17+19). However, the observation of a faster decomposition of 4-NO_2−**1**$^{\bullet-}$ in the presence of the nucleophile permits us to rule out the "reversible classical $S_{RN}1$" route, reactions 0, 12, 15, 16, and

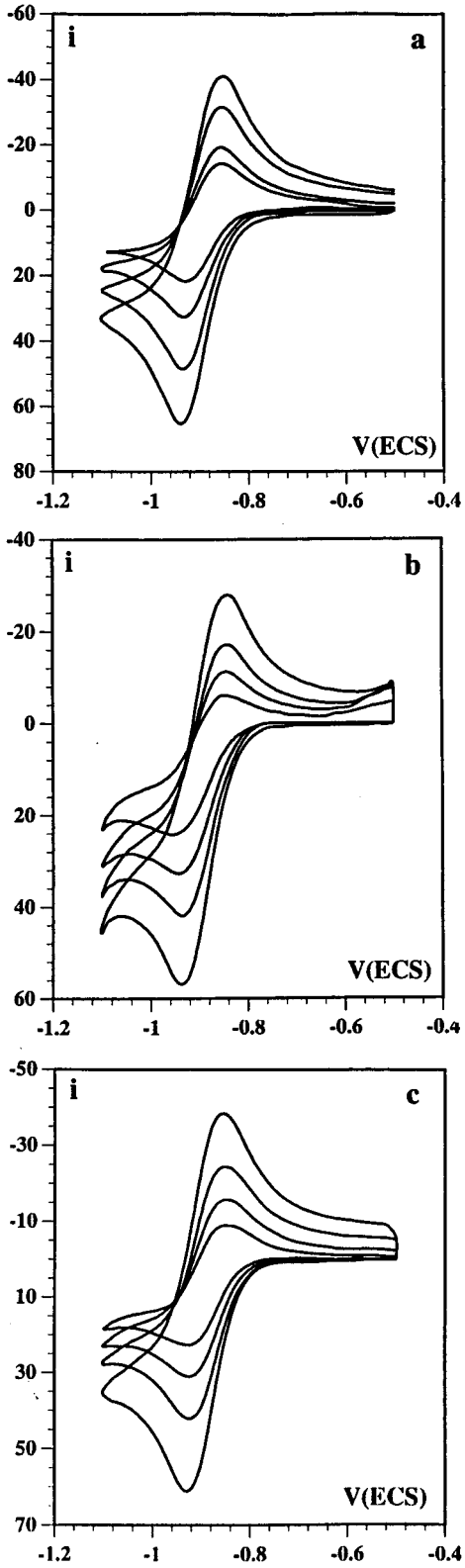

Figure 7. Cyclic voltammetry in ACN + 0.1 M NBu_4BF_4 of (a) (*E*)-4-NO_2−**1** (c^0 = 1.4 mM) and (b) (*E*)-4-NO_2−**1** (c^0 = 1.73 mM) in the presence of malononitrile anion (c^0 = 0.1 M) and (c) (*E*)-4-NO_2−**1** (c^0 = 6 mM) in the presence of cyanide ion (c^0 = 0.647 M).

18, 0+12+15+16+18; in such a case the attack of the nucleophile would intervene after irreversible reaction, 15 and therefore, the rate of decomposition of (*E*)-4-NO_2−**1**$^{\bullet-}$ should not change upon addition of the nucleophile.

A third interpretation of the result of Figure 6 is shown in Scheme 3. It would take into account the elusive $S_{RN}2$ reaction[56,80−87] of which no example has ever be found. An attack of the nucleophile on (*E*)-4-NO_2−**1**$^{\bullet-}$ would form an adduct (reaction 20), the cleavage (reaction 21) of which would lead to the radical anion 1-$CH(CN)_2$−4-NO_2−**2**$^{\bullet-}$ and to the final product **2**−1-$CH(CN)_2$−4-NO_2−**2** along reaction 18.

SCHEME 2: $S_{RN}1$ Reaction with a Reversible Cleavage of the Radical Anion

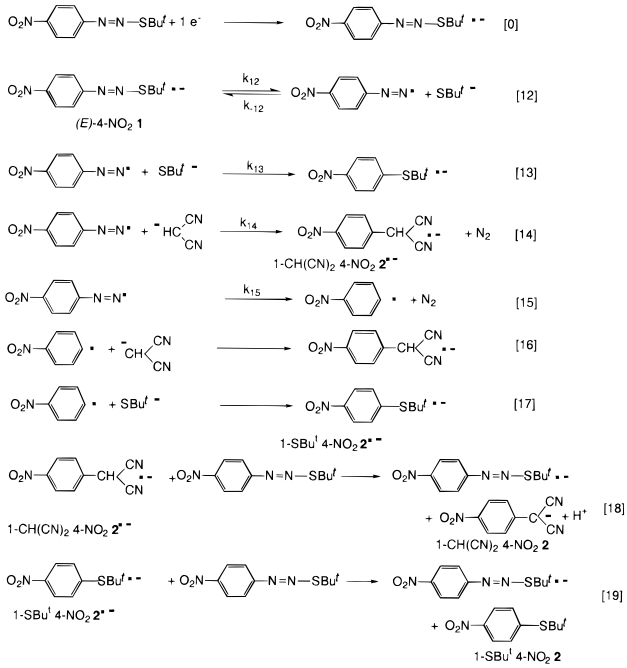

SCHEME 3: $S_{RN}2$ Reaction

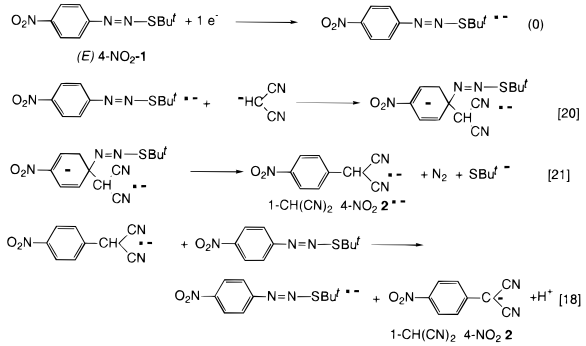

With the "reversible classical $S_{RN}1$" path being excluded, the remaining possibility is therefore either the mechanism consisting of reactions 0, 12, 14, and 18, 0+12+14+18 or an $S_{RN}2$ reaction. To discriminate between these two possibilities, a kinetic analysis of the "reversible nonclassical" $S_{RN}1$ reaction was performed. It is based on the observation that the half-reaction time of the reaction depends linearly on the concentration of the azosulfide. The results of this analysis, the details of which are given in Supporting Information, fit reasonably with the "reversible nonclassical $S_{RN}1$" (reactions 0, 12, 14, and 18, 0+12+14+18) and provide the rate constants that are reported in Table 4 and Scheme 5.

Discussion

The main point that is brought forward by the above experiments is the reversible cleavage of (*E*)-4-NO_2−**1**$^{\bullet-}$. It can explain the fast isomerization of the (*Z*)-isomer through successive cleavage and recombination of the *t*-butanethiolate on the more easily accessible trans position. This is most likely

TABLE 4: Rate and Equilibrium Constants

	4-NO_2−**1**		4-CN−**1**		4-F−**1**	
	(*E*)	(*Z*)	(*E*)	(*Z*)	(*E*)	(*Z*)
k_{12} (s^{-1})	4.1×10^{-2}	6.3×10^{6}	550	4×10^{6}	2×10^{3}	$<8.4 \times 10^{5}$
k_{-12} (M^{-1} s^{-1})	8.9×10^{8}	$<2 \times 10^{10}$	$<4.7 \times 10^{8}$	$<2 \times 10^{10}$	$<2 \times 10^{10}$	$<2 \times 10^{10}$
K_{12} (M)	4.6×10^{-11}	$>6.3 \times 10^{-4}$	$>1.2 \times 10^{-6}$	$>4.2 \times 10^{-5}$	$>1 \times 10^{-7}$	

SCHEME 5

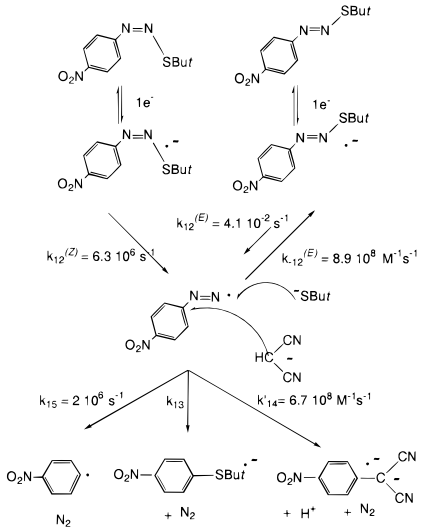

also the case with the 3-NO_2 and 4-CN derivatives for which a slow cleavage of the radical anion and an isomerization are observed. This mechanism, different from the rotation (a)−inversion (b) mechanism, can explain the remarkably much faster rate of isomerization. Starting from the (*E*)-isomer, the recombination giving back (*E*)-4-NO_2−**1**$^{\bullet-}$ proceeds with a rate constant of 8.9×10^{8} M^{-1} s^{-1}, while starting from the (*Z*)-isomer, the isomerization takes place with an overall rate constant of ca. 10^{6} s^{-1}. In view of the above discussion and of Scheme 5, this rate constant must be assigned to $k_{12}^{(E)}$, i.e., to the cleavage of the (*Z*)-isomer radical anion. In any case the cleavage of the radical anion is much faster for the (*Z*)-isomer ($\geq 6.3 \times 10^{6}$ s^{-1}) than for the (*E*)-isomer ($k_{12}^{(E)} = 4.1 \times 10^{-2}$ s^{-1}). From a thermodynamic point of view the equilibrium constants are $K_{12}^{(E)} = k_{12}^{(E)}/k_{-12}^{(E)} = 4.6 \times 10^{-11}$ s and $K_{12}^{(E)} \geq 6.3 \times 10^{-4}$ s (supposing that reaction 12 starting from the (*Z*)-isomer is reversible and taking the rate constant for the recombination to (*Z*)-4-NO_2−**1**$^{\bullet-}$ as k_{diff}). This clearly indicates that the (*E*)-isomer is strongly thermodynamically favored, in agreement with the fact that the (*E*)-isomer is prepared by heating the (*Z*)-isomer in an aprotic solvent. The values for 4-NO_2−**1**, 4-CN−**1**, and 4-F−**1** are summarized in Table 4. Although it is not possible to set even a limit for $K_{12}^{(Z)}$ for 4-F−**1**, it appears that the main changes occur on $k_{12}^{(E)}$, i.e., on the rate of cleavage of the (*E*)-isomer radical anion. This is in line with the very large changes observed for the rate of cleavage of radical anions of aromatic halides.[55]

A cleavage recombination mechanism had already been proposed[49] for the thermal isomerization of azosulfides, but the cleavage was supposed to occur in an heterolytic fashion, which as we know now is unlikely in the case of a thermal cleavage and of course not possible in the case of an electrochemical reduction. Also related, in a looser fashion, the addition−elimination mechanism is used in fine organic synthesis for the isomerization of olefins.[88]

Even if the cleavage recombination mechanism can be put on a firm basis, one can wonder if a rotation mechanism could take place in parallel (we do not consider the inversion mechanism c for which calculations indicate a much higher activation barrier). Neither the measurements of spin densities nor the estimation of the activation barrier make unlikely the occurrence of a rotation mechanism in the case of 4-NO_2−**1**. The best answer that can be given with the available experimental data is that if the first-order rotation was taking place with a significant rate, the half-life time of the radical anion should not vary with the concentration.

SCHEME 6

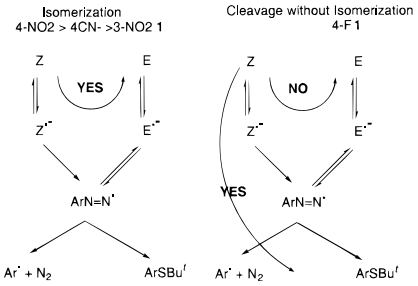

Concerning the other azosulfides investigated in this paper (4-F−**1**, 3-F−**1**, 2,4,6-Me_3−**1**), no isomerization can be observed by cyclic voltammetry or by spectroelectrochemistry. At high scan rates, one observes the cleavage of the (*Z*)-isomer but not the recombination to the (*E*)-isomer. This must be related to a lower rate of the attack of the same *t*-butanethiolate nucleophile on the nitrogen of the diazenyl radical (the equivalent of k_{-12} in Scheme 2). For 4-H−**1**, 4-Bu^t−**1**, and 4-MeO−**1**, the cleavage of the radical anion and the recombination seem to have comparable rates.

This reversible cleavage also bears consequences on the $S_{RN}1$ mechanism of azosulfides. We had already stated[64] that the intermediacy of aryldiazenyl radicals along the fragmentation of **1**$^{\bullet-}$ could be disregarded, since its rate of cleavage is too slow[89,90] to account for the very fast reaction of the "internal" nucleophile. On the other hand, it is unlikely that a concerted cleavage would occur at the level of the radical anion; even for azomethane the photochemical cleavage has been shown to be stepwise,[92] and aryldiazenyl radicals are sufficiently stable to be observed by ESR.[89,90] A possible way to reconcile these facts is to propose that the attack of the *t*-butanehiolate takes place in solution on the carbon atom of the diazenyl radical, as we had already proposed in the gas phase.[66] This can be summarized as in Scheme 5.

Conclusions

The unusually fast (*Z*) to (*E*) isomerization initiated by the one-electron reduction of 4-nitrophenylazo *tert*-butylsulfide is related to the occurrence of the reversible cleavage of the radical anion. Other azosulfides with less electron-withdrawing substituents cleave faster than they isomerize. The different behaviors in the absence of "external nucleophile" are summarized in Scheme 6. During a slow scan rate cyclic voltammetry of 4-NO_2−**1**, 4-CN−**1** and 3-NO_2−**1** isomerize while 4-F−**1** cleaves faster than it isomerizes.

This reversible cleavage of azosulfides renders necessary a modification of the $S_{RN}1$ mechanism of azosulfides. In view of

the mechanism proposed in Scheme 5, one can reexamine the reduction of (*E*)-4-cyanophenylazo phenylsulfide for which we had concluded that the recombination of the aryl radical and the phenyl thiolate takes place in the solvent cage.[65] It should be noted that this conclusion was reached through different methods, one of which (competition between the "internal" phenyl thiolate nucleophile and the "external" cyanide nucleophile and the observation that a fraction of the radicals could not be trapped by the "external" nucleophile) did not rely on mechanistic assumptions. The cleavage of the 4-cyanophenyldiazenyl radical can also be obtained from the work of Suehiro,[89,90] $k = 4.7 \times 10^5$ s^{-1}. Therefore, if the cleavage of this radical was a step in the mechanism, the overall rate constants should not exceed this value and no cage effect could be observed with this compound. Besides, as stated above, recent femtosecond chemistry results[91] make unlikely the simultaneous cleavage of the CN and CS bonds. Therefore, the cage recombination in solution should be the attack of the phenyl thiolate on the carbon of the diazenyl with further cleavage of dinitrogen, as had been postulated in the gas phase.[66] It can be concluded that at least part of the substituted products should be the result of an attack on the diazenyl radical and not exclusively, as postulated before, of an attack on the ensuing aryl radical. In addition, it is possible to rule out the existence of an $S_{RN}2$ reaction in a case where its occurrence seemed more likely than ever.

Experimental Section

The spectroelectrochemical cell based on a gold LIGA structure has been described previously.[70−73] The spectra were recorded with a fast-scanning (maximum speed of 3 ms/spectrum) diode array spectrometer (J. & M. Analytische Mess- und Regeltechnik Gmbh, Aalen, Germany). The 75 W xenon lamp and the spectrophotometer were connected by optical waveguides with the LIGA cell. The reference was an Ag/AgCl electrode standardized against the ferrocene/ferrocenium couple. To minimize photochemical isomerization in the course of the electrochemical experiments (see later), the light intensity was decreased by placing the optical waveguides at a proper distance from the entrance of the cell and keeping the shutter of the spectrophotometer closed between the recording of successive spectra.

The ESR spectra were recorded as described previously.[74]

Low scan rate cyclic voltammograms were recorded on 1 mm gold or 0.8 mm glassy carbon electrodes using a homemade potentiostat. A homemade program using a DA−AD card[70] drove the potentiostat and recorded the current data.

For high scan rate cyclic voltammetry, the microelectrode was a gold wire (10 μm diameter) sealed in soft glass.[92] The signal generator was a Hewlett-Packard 3314A, and the curves were recorded using a 4094 Nicolet oscilloscope with a minimum acquisition time of 5 ns/point.

Acetonitrile (0.005% water) and the supporting electrolyte tetrabutylammonium perchlorate were used without further purification. Both (*E*)- and (*Z*)-azosulfides were synthesized as previously reported.[48,59,66]

The charge and spin density and energy calculations were performed using the PC-Spartan software 1.1 (Wavefunction Inc., Irvine, CA) for AM1 calculations and the Gaussian 94w package[78] for DFT calculations.

The 4-nitrophenyl *tert*-butylsulfide, the reduction product of 4-NO_2−**1**, has been previously identified.[52]

An electrolysis of 4-F−**1** was performed in order to identify the final reduction products. Samples of 85 mg of 4-F−**1** dissolved in 10 mL of ACN + 0.1 M NEt_4BF4 in a glassy carbon crucible (c = 40 mM) were electrolyzed at −1.80 V/SCE. At the end of the electrolysis, after consumption of 1.3 F/mol, the solution was poured in 10 mL of dichloromethane and extracted with 3 × 10 mL of water to remove the supporting electrolyte. The organic layer was dried over $MgSO_4$ and evaporated to give 51 mg of a brown uncrystallized product. This product shows a UV spectrum (λ_{max} = 240 nm with a shoulder at 273 nm and a residual absorption at 297 nm), indicating, by comparison with the final spectrum (λ_{max} = 297 nm) observed in spectroelectrochemistry, a further evolution of the solution during the electrolysis. The NMR spectrum of the mixture shows a complex spectrum where the ratio of aliphatic to aromatic protons is somewhat higher (2.38) than in the starting 4-F−**1** (2.25). This is likely due to the loss of fluorobenzene (bp = 85.1 °C) in the stream of nitrogen used to deoxygenate the solution. A GC mass analysis of the solution indicates the presence of the expected 4-fluorophenyl *tert*-butylsulfide, of fluorobutylbenzene, of $FC_6H_4SCH_2Cl$ most likely resulting from the nucleophilic reaction of 4-fluorophenyl thiolate (obtained from the cleavage of the radical anion of 4-fluorophenyl *tert*-butylsulfide) with dichloromethane used during the workup of the electrolysis, of $FC_6H_4SC_6H_4$ likely resulting from the reaction of a 4-fluorophenyl radical with 4-fluorophenyl thiolate and of di-*tert*-butyl disulfide obtained by reoxidation during the workup of the corresponding thiolate.

An electrolysis of (*E*)-4-NO_2−**1** (0.869 mM) in the presence of the malononitrile anion tetramethylammonium salt $(CN)_2CH^-$ (8.15 mM) in ACN + 0.1 M NEt_4BF4 in a glassy carbon crucible consumed 1.5 F/mol. The final solution was analyzed by HPLC (25 cm C8 column eluted with MeOH/H_2O at 0.8 mL min^{-1}), and detection was performed by recording successive spectra with the fast-scanning spectrophotometer described above. The final product 1-$CH(CN)_2$4-NO_2−**2** is very acidic ($pK_{HA} \approx -1$ in DMSO[79]) and exists mainly as its conjugated base in ACN. To be certain that all of the the compound is in basic form, tetramethylammonium was added before titration. The yield of 1-$CH(CN)_2$−4-NO_2−**2** is 61%, with only 2% of the starting compound and less than 1% of 4-nitrophenyl *t*-butylsulfide remaining.

Acknowledgment. A.N. gratefully acknowledges a fellowship from Deutsche Forschunggemeinschaft (DFG). We are grateful to Nelson Novo for performing some of the experiments and to Dr A. Rockenbauer for permission to use the ESR analyzing program EPR.

Supporting Information Available: Description containing the kinetic analysis, Scheme 4, and Appendixes 1 and 2 on the $S_{RN}1$ reaction path, and Figure 8 showing the half reaction time of 4-NO_2−**1** vs initial concentration of (E)-4-NO_2−**1**. This material is available free of charge via the Internet at http://pubs.acs.org.

References and Notes

(1) Saremi, F.; Teke, B. *Adv. Mater.* **1998**, *10*, 388.
(2) Liu, Z. F.; Fujishima, A.; Hashimoto, K. *Nature* **1990**, *347*, 648.
(3) Kampf, G. *Ber. Bunsen-Ges. Phys. Chem.* **1985**, *89*, 1179.
(4) Seki, T.; Sakuragi, M.; Kawanishi, Y.; Suzuki, Y.; Tamaki, T.; Fukuda, R.; Ichimura, K. *Langmuir* **1993**, *9*, 211.
(5) Nakagawa, M.; Rikukawa, M.; Watanabe, M.; Sanui, K.; Ogata, N. *Bull. Chem. Soc. Jpn.* **1997**, *70*, 737.
(6) Gilat, S. L.; Kawai, S. H.; Lehn, J. M. *J. Chem. Soc., Chem. Commun.* **1993**, 1439.
(7) Kawai, S. H.; Gilat, S. L.; Lehn, J. M. *J. Chem. Soc., Chem. Commun.* **1994**, 1011.
(8) Iyoda, T.; Saika, T.; Honda, K.; Shimidzu, T. *Tetrahedron Lett.* **1989**, *30*, 5429.

(9) Saika, T.; Iyoda, T.; Honda, K.; Shimidzu, T. *J. Chem. Soc., Perkin Trans 2* **1993**, 1191.
(10) Saika, T.; Irie, M.; Shimidzu, T. *J. Chem. Soc., Chem. Commun.* **1994**, 2123.
(11) Zhi, J. F.; Baba, R.; Hashimoto, K.; Fujishima, A. *Ber. Bunsen-Ges. Phys. Chem.* **1995**, *99*, 32.
(12) Zhi, J. F.; Baba, R.; Hashimoto, K.; Fujishima, A. *Chem. Lett.* **1994**, 1521.
(13) Liu, Z. F.; Hashimoto, K.; Fujishima, A. *Nature* **1990**, *347*, 658.
(14) Liu, Z. F.; Loo, H.; Baba, R.; Fujishima, A. *J. Electroanal. Chem.* **1989**, *270*, 437.
(15) Newall, A. K.; Utley, J. H. P. *J. Chem. Soc., Chem. Commun.* **1992**, 800.
(16) Achatz, J.; Fischer, C.; Salbeck, J.; Daub, J. *J. Chem. Soc., Chem. Commun.* **1991**, 504.
(17) *Photochromism, Molecules and Systems*, H. Dürr, Bouas-Laurent, H. Eds., Elsevier: Amsterdam, 1990.
(18) Rau, H. In *Photochemistry and Photophysics*; Rabek, J. F. Ed.; CRC Press Inc.: Boca Raton, 1990; p 119.
(19) Zimmermann, G.; Chow, L. Y.; Paik, U.-J. *J. Am. Chem. Soc.* **1958**, *80*, 3528.
(20) Rau, H.; Lüddecke, E. *J. Am. Chem. Soc.* **1982**, *104*, 1617 and references therein
(21) Monti, S.; Orlandi, G.; Palmieri, P. *Chem. Phys.* **1982**, *71*, 87.
(22) Nägele, T.; Hoche, R.; Zinth, W.; Wachtevil, *J. Chem. Phys. Letter* **1997**, *272*, 489.
(23) Le Fèvre, R. J. W.; Northcott, J. *J. Chem. Soc.* **1953**, 857.
(24) Schulte-Frohlinde, D. *Justus Liebig Ann. Chem.* **1958**, *612*, 131.
(25) Tsuda, M.; Kuratany, K. *Bull Chem. Soc. Jpn.* **1964**, *37*, 1284.
(26) Halicioglu, T.; Sinanoglu, O. *N. Y. Acad. Sci.* **1969**, 308.
(27) Wildes, P. D.; Pacifici, J. G.; Irick, G.; Whitten, D. G. *J. Am. Chem. Soc.* **1971**, *93*, 2004.
(28) Haberfield, P.; Block, P. M.; Lux, S. M. *J. Am. Chem. Soc.* **1975**, *97*, 5804.
(29) Nerbonne, J. M.; Weiss, R. J. *J. Am. Chem. Soc.* **1978**, *100*, 5953.
(30) Binenboim, J.; Burcat, A.; Lifshitz, A.; Shamir, J. *J. Am. Chem. Soc.* **1966**, *88*, 5039.
(31) Talaty, E. R.; Fargo, J. C. *Chem. Comm.* **1967**, *2*, 65.
(32) Sueyoshi, T.; Nishimura, N.; Yamamoto, S.; Hasegawa, S. *Chem. Lett.* **1974**, 1131.
(33) Braun, E. V.; Granneman, *J. Am. Chem. Soc.* **1975**, *97*, 621.
(34) Nishimura, N.; Sueyoshi, T.; Yamanaka, H.; Imai, E.; Yamamoto, S.; Hasegawa, S. *Bull. Chem. Soc. Jap.* **1976**, *49*, 1381.
(35) Wolf, E.; Camenga, H. K. *Z. Phys Chem.* **1977**, *107*, 21.
(36) Klopman, G.; Doddapaneni, N. *J. Phys. Chem.* **1974,** *78*, 1825.
(37) Laviron, E.; Mugnier, Y. *J. Electroanal. Chem.* **1978**, *93*, 69.
(38) Degrand, C.; Belot, G. *Electrochim. Acta* **1978**, *21*, 71.
(39) Gescheidt, G.; Lamprecht, A.; Heinze, J.; Schüler, B.; Schmittel, M.; Kiau, S.; Rüchardt, C. *Helvetica Chimica Acta* **1992**, *75* , 1607.
(40) Dietz, R.; Peover, M. E. *Discuss. Faraday Soc.* **1968**, *45*, 154.
(41) Jensen, B. S.; Lines, R.; Pasberg, P.; Parker, V. D. *Acta Chem. Scand., B* **1977**, *31*, 707.
(42) Knorr, A.; Daub, J. *Angewandte Chem. Int Ed. Eng.* **1995**, *34*, 2664.
(43) Chien, C. K.; Wang, H. C.; Swarc, M.; Bard, A. J.; Itaya, K. *J. Am. Chem. Soc.* **1980**, *102*, 3100.
(44) (a) Bard, A. J.; Puglisi, V. J.; Kenkel, J. V.; Lomax, A. *Faraday Discuss. Chem. Soc.* **1973,** *56*, 353. (b) Yeh, L. S.; Bard, A. J. *J. Electrochem. Soc.* **1977**, *124*, 189.
(45) (a) Yeh, L. S.; Bard, A. J. *J. Electroanal. Chem.* **1976**, *70*, 157. (b) Yeh, L. S.; Bard, A. J. *J. Electroanal. Chem.* **1977**, *81*, 333.
(46) Mabon, G.; Le Guillanton, G.; Simonet, J. *J. Electroanal. Chem.* **1981**, *130*, 387.
(47) Mabon, G.; Simonet, J. *Electrochim Acta* **1992**, *37*, 2467.
(48) Dell'Erba, C.; Novi, M.; Petrillo, G.; Tavani, C.; Bellandi, P. *Tetrahedron* **1991**, *47*, 333.
(49) van Zwet, H.; Kooyman, E. C. *Recueil Trav. Chim. Pays-Bas* **1967**, *86*, 993.
(50) van Beek, L. K. H.; van Beek, J. R. G. C. M.; Boven, J.; Schoot, C. J. *J. Org. Chem.* **1971**, *36*, 2195.
(51) Broken-Zijp, J.; van der Bogaert, H. *Tetrahedron* **1973**, *29*, 4169.
(52) Hapiot, P.; Neudeck, A.; Pinson, J.; Novi, M.; Petrillo, G.; Tavani, C. *J. Electroanal Chem.* **1996**, *422*, 99.
(53) Bunnett, J. F. *Acc. Chem. Res.* **1978**, *11*, 413.
(54) Rossi, R. A.; Rossi, R. H. In *Aromatic Nucleophilic Substitution by the $S_{RN}1$ Mechanism*; A. C. S. Monograph 178, American Chemical Society, Washington, D. C., 1983.
(55) Pinson, J.; Savéant, J. M. In *Electroorganic Synthesis, Festschrift for Manuel M.; Baizer*; Electrochemical Induction of SRN1 Nucleophilic Substitution. Edited by Little, R.D and Weinberg, N. L.; Marcel Dekker: New York, 1991; p 29.
(56) Savéant, J. M. *Tetrahedron* **1994**, *50*, 10117.
(57) Petrillo, G.; Novi, M.; Garbarino, G.; Dell'Erba, C. *Tetrahedron* **1986**, *42*, 4007.
(58) Petrillo, G.; Novi, M.; Garbarino, G.; Dell'Erba, C. *Tetrahedron* **1987**, *43*, 4625.
(59) Petrillo, G.; Novi, M.; Tavani, C.; Berta, G. *Tetrahedron* **1990**, *46*, 7977.
(60) Dell'Erba, C.; Novi, M.; Petrillo, G.; Tavani, C. *Tetrahedron* **1992**, *48*, 325. Dell'Erba, C.; Novi, M.; Petrillo, G.; Tavani, C. *Tetrahedron* **1994**, *50*, 3529.
(61) Dell'Erba, C.; Novi, M.; Petrillo, G.; Tavani, C. *Tetrahedron* **1993**, *49*, 235.
(62) Pinson, J.; Savéant, J.-M. *J. Chem. Soc., Chem. Commun.* **1974**, 933.
(63) Savéant, J.-M. *Acc. Chem. Res.* **1980**, *13*, 123.
(64) Savéant, J.-M. *Adv. Phys. Org. Chem.* **1990**, *26*, 1.
(65) Dell'Erba, C.; Houmam, A.; Novi, M.; Petrillo, G.; Pinson, J. *J. Org. Chem.* **1993**, *58*, 2670.
(66) Dell'Erba, C.; Houmam, A.; Morin, N.; Novi, M.; Petrillo, G.; Pinson, J.; Rolando, C. *J. Org. Chem.* **1996**, *61*, 929.
(67) M'Halla, F.; Pinson, J.; Savéant, J. M. *J. Am. Chem. Soc.* **1980**, *102*, 4120.
(68) Amatore, C.; Pinson, J.; Savéant, J. M.; Thiébault, A. *J. Am. Chem. Soc.* **1982**, *104*, 817.
(69) Rudolf, M.; Feldberg, S. W. *Digisim 2.0, Cyclic Voltammetric Simulator for Windows*; Bioanalytical Systems Inc.: West Lafayette, IN, 1996.
(70) Neudeck, A.; Dunsch, L. *J. Electroanal. Chem.* **1994**, *370*, 17.
(71) Neudeck, A.; Dunsch, L. *J. Electroanal. Chem.* **1995**, *386*, 138.
(72) Neudeck, A.; Dunsch, L. *Electrochim. Acta* **1995**, *40*, 1427.
(73) Neudeck, A.; Kress, L. *J. Electroanal. Chem.* **1997**, *437*, 141.
(74) Petr, A.; Dunsch, L.; Neudeck, A. *J. Electroanal. Chem.* **1996**, *412*, 153.
(75) Rockenbauer, A.; Korecz, L. *Appl. Magn. Reson.* **1996**, *10*, 29.
(76) Rockenbauer, A.; Korecz, L. *J. Chem. Soc., Perkin Trans. 2* **1993**, 2149.
(77) Rieger P. H.; Fraenkel, G. K. *J. Chem. Phys.* **1963**, *39*, 609.
(78) Frisch, M. J.; Trucks, G. W.; Schlegel, H. B.; Gill, P. M. W.; Johnson, B. G.; Robb, M. A.; Cheeseman, J. R.; Keith, T.; Peterson, G. A.; Montgomery, J. A.; Ragavachari, K.; Al-Laham, M. A.; Zakrewski, V. G.; Ortiz, J. V.; Foresman, J. B.; Cioslowski, J.; Stefanov, B. B.; Nanayakkara, A.; Challacombe, M.; Peng, C. Y.; Ayala, P. Y.; Chen, W.; Wong, M. W.; Andres, J. L.; Replogle, E. S.; Gomperts, R.; Martin, R. L.; Fox, D. J.; Baker, J.; Stewart, J. P.; Head-Gordon, M.; Gonzalez, C.; Pople, J. A. *Gaussian 94*, revision E.1; Gaussian Inc.: Pittsburgh, PA, 1995.
(79) Throughton, E. B.; Molter, K. E.; Arnett, E. M. *J. Am. Chem. Soc.* **1984**, *106*, 6726.
(80) Denney, D. B.; Denney, D. Z. *Tetrahedron* **1991**, *47*, 6577.
(81) Denney, D. B.; Denney, D. Z.; Perez, A. J. *Tetrahedron* **1993**, *49*, 4463.
(82) Bunnett, J. F. *Tetrahedron* **1993**, *49*, 4477.
(83) Rossi, R. A.; Palacios, S. M. *Tetrahedron* **1993**, *49*, 4485.
(84) Marquet, J.; Jiang, Z.; Gallardo, I.; Battle, A.; Cayon, E. *Tetrahedron Lett.* **1993**, *34*, 2801.
(85) Mir, M.; Espin, M.; Marquet, J.; Gallardo, I.; Tomasi, C. *Tetrahedron Lett.* **1994**, *35*, 9055.
(86) Niat, M.; Marquet, J.; Jiang, Z.; Gallardo, I.; Cervera, M.; Mir, M. *Tetrahedron Lett.* **1994**, *35*, 9059.
(87) Balslev, H.; Lund, H. *Tetrahedron* **1994**, *50*, 7889.
(88) Chatgilialoglu, C.; Ballestri, M.; Ferreri, C.; Vecchi, D. *J. Org. Chem.* **1995**, *60*, 3826 and references therein.
(89) Suehiro, T.; Masuda, S.; Tashiro, T.; Nakausa, R.; Taguchi, M.: Koike, A.; Rieker, A. *Bull. Chem. Soc. Jpn.* **1986**, *59*, 1887.
(90) Suehiro, T.; Masuda, S.; Nakausa, R.; Taguchi, M.; Mori, A.; Koike, A.; Date, M. *Bull. Chem. Soc. Jpn.* **1987**, *60*, 3221.
(91) Diau, E. W. G.; Abou-Zied, O. K.; Scala, A. A.; Zewail, A. H. *J. Am. Chem. Soc.* **1998**, *120*, 3245.
(92) Andrieux, C. P.; Garreau, D.; Hapiot, P.; Pinson, J.; Savéant, J. M. *J. Electroanal. Chem.* **1988**, *243*, 321.
(93) Erentova, K.; Adamcik, V.; Stasko, A.; Nuyken, A.; Lang, A.; Leitner, M. *Collect. Czech. Chem. Commun.* **1997**, *62*, 855.
(94) Rapta, P.; Stasko, A.; Bustin, D.; Nuyken, O.; Voit, B. *J. Chem. Soc., Perkin Trans. 2* **1992**, 2049.
(95) Geels, E. G.; Konaka, R.; Russell, G. A. *Chem. Commun.* **1965**, 13.
(96) Strom, E. T.; Russell, G. A.; Konaka, R. *J. Chem. Phys.* **1965**, *42*, 2033.
(97) Russell, G. A.; Konaka, R.; Strom, E. T.; Danen, W. C.; Chang, K. Y.; Kampp, G. *J. Am. Chem. Soc.* **1968**, *90*, 4646.
(98) Neugebauer, F. A.; Weger, H. *Chem. Ber.* **1975**, *108*, 2703.
(99) Gulick, W. M.; Schwartz, G. L.; Parrish, R. S. *J. Magn. Reson.* **1976**, *22*, 81.